Termomechanical Analysis of 3D Printing Specimens (Acrylonitrile Butadiene Styrene)

Juan Atonal-Sánchez, Juan Alfonso Beltrán-Fernández, Luis Héctor Hernández-Gómez, Luz Yazmin-Villagran, Juan Alejandro Flores-Campos, Adolfo López-Lievano and Pablo Moreno-Garibaldi

Abstract In the present work the thermomechanical properties of acrylonitrile butadiene styrene (ABS) were evaluated at ambient and higher temperatures. The test specimens were previously modeled in a computer aided design (CAD) program (SolidWorks) with standardized dimensions according to the D638 Standard of the American Society for Testing Materials (ASTM) (ASTM in D638-10 Standard Test Method for Tensile Properties of Plastics, 2012). These models were exported to computer aided manufacturing (CAM) software for later 3D printing. The 3D printer used is based on fused deposition modeling (FDM) technology. The impressions were configured with a distance of 0.3 mm between layers and angles of 45° and 135° from the horizontal axis. Experimental tests were performed at a speed of 10 mm/min on a universal testing machine (Shimadzu AG-I) with the aid of a support and control system for the band-type electrical resistance, that was used as a heat source, as well

J. Atonal-Sánchez (✉) · J. A. Beltrán-Fernández · L. H. Hernández-Gómez
J. A. Flores-Campos · A. López-Lievano · P. Moreno-Garibaldi
Instituto Politécnico Nacional - Escuela Superior de Ingeniería Mecánica y Eléctrica, Sección de Estudios de Posgrado e Investigación Edificio 5. 2do Piso, Unidad Profesional Adolfo López Mateos "Zacatenco" Col. Lindavista, C.P. 07738 Ciudad de Mexico, Mexico
e-mail: juan_atonal@hotmail.com

J. A. Beltrán-Fernández
e-mail: jbeltranf@hotmail.com

L. H. Hernández-Gómez
e-mail: luishector56@hotmail.com

J. A. Flores-Campos
e-mail: jaflores@ipn.mx

A. López-Lievano
e-mail: k_lievano@hotmail.com

P. Moreno-Garibaldi
e-mail: pmg170588@gmail.com

L. Yazmin-Villagran
Facultad de Ingeniería Mecánica y Eléctrica, Universidad Veracruzana, Prolongación Venustiano Carranza S/N, Col. Revolución, 93390 Poza Rica, Veracruz, Mexico
e-mail: yazvillagranv@gmail.com

as an infrared pyrometer to make temperature measurements during the tensile test. Finite element analyses were performed with the help of the ANSYS software using the SolidWorks generated model, which was imported with the file format[*]. IGS for further study. The results obtained from the experimental tests and numerical simulations differ, because the Poisson´s ratio and the coefficient of thermal expansion remained constant for the numerical analyses.

Keywords 3D printing · Fused deposition modeling (FDM) · Finite element method (FEM) · Ultimate stress · Modulus of elasticity · Thermal expansion coefficient

1 Introduction

In recent years, many sectors have become great consumers of polymers. One of the most used polymers in engineering applications is ABS. Characterized by easy reprocessing, low cost, high impact and mechanical and chemical resistance [2].

The mechanical properties of solid materials used in engineering designs are determined by destructive mechanical testing [3]. For some years destructive tests have been reduced less and less, at present, numerical simulation based on the finite element method (FEM) has taken more relevance every day, decreasing conventional tests.

There are standardized tests governed by associations, where the dimensions of the specimen are established for each type of test, either of tension, compression, torsion, flexion, among others. Different 3D printing technologies have been developed and continue to evolve for the generation of parts.

The materials that can currently be used for 3D printing are varied and the fact is that they greatly influence the cost of printing [4]. The most widely used thermoplastics in FDM printers is ABS and polylactic acid (PLA) [5]. ABS is the plastic studied in this work.

As is well known, many of these parts are subjected to different states of loading in different applications, so that the proper selection of the material of each of them is based mainly on their mechanical properties.

On the other hand, the ABS characterization depends on the criteria of printing (orientation of fibers, distance between layers, percentage of compaction), these configurations of impression alter the resistance and it is reflected in the performance of the work to which it will be applied.

The mechanical behavior of the materials under different states of loading is still studied and generally thermal fluence experiments are used to analyze and predict the behavior of the materials at different temperatures [6]. Therefore, it is essential to know and understand in detail the thermo-mechanical properties of ABS.

2 Finite Element Method

The FEM has been generally applied structurally, however, advances in this field have been able to include heat transfer for which two types of thermal analyses were developed, one "stable", which does not consider time as a factor in the analysis and the other type is the "transient" analysis, in which the conditions are variable in time.

In the case of thermal analysis, it is necessary to create a discrete model of the parts to be analyzed, so we proceed to a division of geometry into a finite number of elements, which in turn are defined by nodes, and in this way, it is possible to establish the responses generated by each element attached to another through its nodes.

There are many elements in the libraries of each program based on the FEM that adapt to the type of analysis to study, which in the case of ANSYS are the element types beam, solid, shell, among others.

SHELL181 is suitable for analyzing thin or moderately thick structures. It is an element of four nodes with six degrees of freedom in each node: translations in the X, Y, Z, and rotations on the X, Y, and Z axes. The option of triangular elements should only be used as filler elements in the mesh generation.

Figure 1 shows the geometry, location of the nodes, and the coordinate system for this. The element is defined by four nodes: I, J, K, and L.

Temperatures can be introduced as loads to the element at the 1–8 corners. The first corner temperature T1 is set by default to the uniform temperature (TUNIF). The other temperatures, if not specified acquire the temperature T1.

This element has the characteristic of generating layers with orientations that allows simulating the printed specimens in ABS.
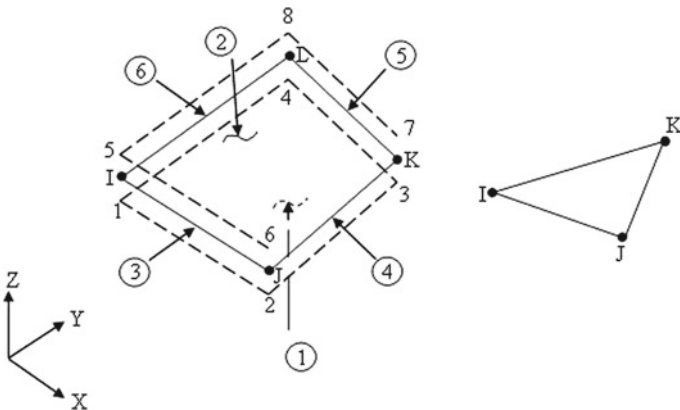

Fig. 1 Shell181, geometry, nodes and coordinates

3   3D Printing

3D printing has gained a lot of popularity in recent years, owing to the interest consumers have had for low-cost 3D printers. Many sectors such as medicine, engineering, architecture, aerospace, the automotive industry and many others are the main areas of application for this innovative printing device [7].

When talking about 3D printing several terms appear to be used interchangeably: rapid prototyping, fast manufacturing or additive manufacturing. These terms used are erroneously because not all printers have the same technology. Rapid prototyping, based on the definition of Ian Gibson, is the process of creating a part or system quickly before its commercialization [8].

There are several technologies used in 3D printers, the main difference is in the way each layer is put to create the piece. Table 1 shows some of these technologies.

For the generation of the used specimens, the tensile tests were produced with a da Vinci 3D printer based on the FDM technology. This 3D printer creates parts layer by layer from bottom to top by heating and extruding the thermoplastic filament. The procedure is as follows:

- The 3D CAD file is placed in the CAM software. The trajectory is then plotted to extrude the thermoplastic material.
- The 3D printer heats the thermoplastic material until it reaches a semiliquid state and deposits it into ultra-fine droplets along the extrusion path.
- The material is removed.

3.1   Printing Material (ABS)

The production of plastics exceeds that of metals and continues to expand on a large scale. Plastics are divided into two groups: the first is made up of thermostatic polymers and the second, the largest, the thermoplastic polymers [9].

Table 1   3D printing technologies

Technology	Materials used
Selective laser sintering (SLS)	Thermoplastics, Metallic powders, ceramic powders
Direct sintering in metal by Laser (DMLS)	Metal alloys
Modeling by Molten Deposition (FDM)	Thermoplastics and Eutectic Metals
Stereolithography (SLA)	Photopolymers
Manufacture of objective by laminate (MOL)	Paper, film, plastics
Fused by electronic beam (EBM)	Titanium alloys
3D printing by powders and inkjet (PP)	Gypsum

Fig. 2 ABS filament for 3D printing

Acrylonitrile butadiene styrene is a thermoplastic polymer composed of three types of monomers. Acrylonitrile, butadiene and styrene (see Fig. 2) that when combined they result in one of the most widely used synergies in the world of commercial polymers.

The result of this combination is another polymer with final properties of the base polymers. With this fusion a great chemical resistance is achieved, such as resistance to fatigue, hardness and stiffness thanks to acrylonitrile. On the other hand butadiene, which is an elastomeric component, provides good tenacity and resistance to impact. Styrene for its part provides resistance to heat, increases its processability, hardness and stiffness, and allows the addition of color. Its molecular formula is (C_8H_8–C_4H_6–C_3H_3N) which represents the monomer that constitutes ABS.

Most ABS resins usually contain 21–27% acrylonitrile, 12–25% butadiene and 54–63% styrene. Today more as a product for 3D ABS has been increasingly extended in diverse sectors and introduced for 3D printing for mechanical and biomedical applications in order to evaluate the final models [10–13].

3.2 Heat Source

Although there are a wide variety of devices for heat generation, the one used in this study was an electrical resistance band type. This device that provides energy in the form of heat in various types of processes is generated by cylindrical surface elements.

The band-type resistance has a hollow cylindrical shape; different models were considered according to the specifications of each project. The manufacture of a band resistance is based on the characteristics of the process to be heated, dimensions, assembly and electrical capacities, for this there are three forms of manufacture used:

- Resistance Type Mica Band
- Band-type resistance with mineral insulation
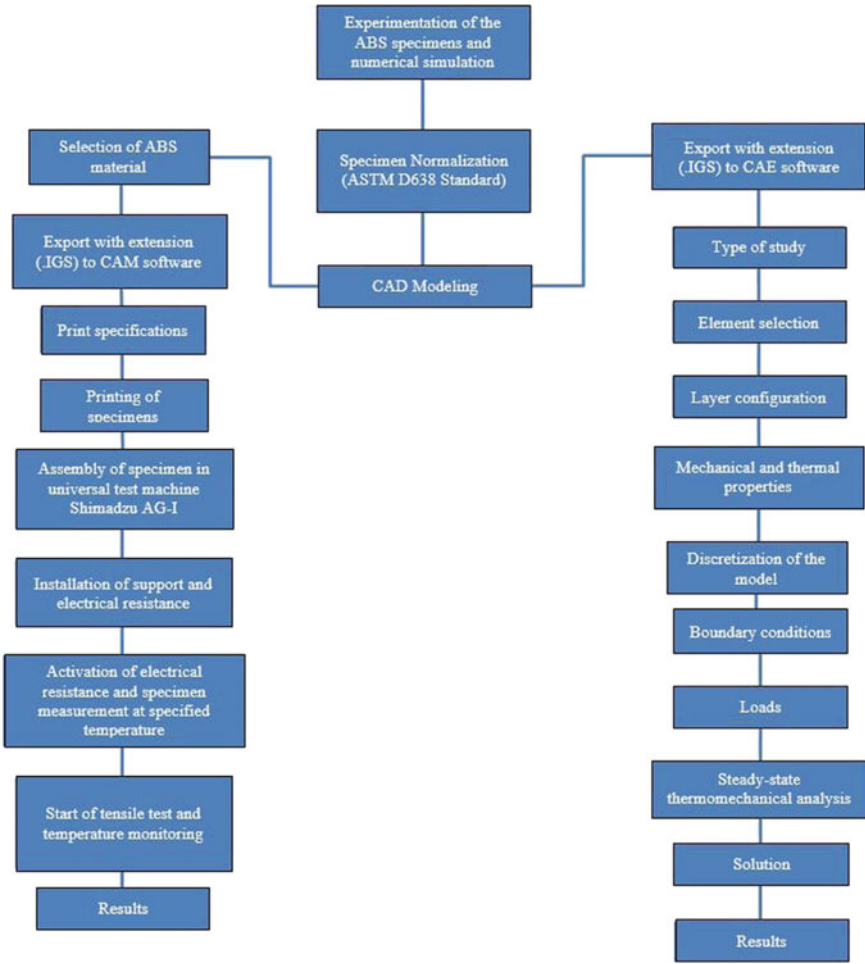- Band-type resistance with ceramic element.

Fig. 3 Stages of experimental and numerical development

4 Experimentation

Before beginning to explain the experimentation developed and the materials used in 3D printing, as well as the auxiliary devices, a diagram (Fig. 3) of the process that was followed during the experimentation is presented.

The specimen model was generated with standardized measurements established by ASTM D638 for tensile tests on flat test specimens (Fig. 4).

The standard establishes the following dimensions for the specimen:

W	Width of the narrow zone	6 mm
L	Length of the narrow zone	33 mm
WO	Width of ends	19 mm
LO	Total length	115 mm
G	Calibrated length	25 mm
D	Distance between jaws	65 mm
R	Radio	14 mm
T	Thickness	4 mm

Defined the dimensions of the specimen the model was generated. In this case, the Solidworks 2015 design program was used for this purpose (Fig. 5).

The part was modeled in SolidWorks, and exported with extension (IGS) to CAM software, which is connected to the da Vinci 1.0 printer with FDM technology. Before
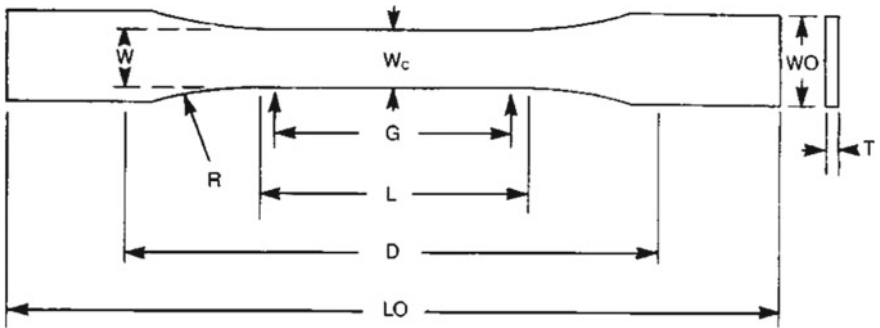
Fig. 4 Standardized specimen according to ASTM D638

Fig. 5 Three-dimensional model

Fig. 6 ABS Printed specimens

Fig. 7 Filament directions 45° and 135°
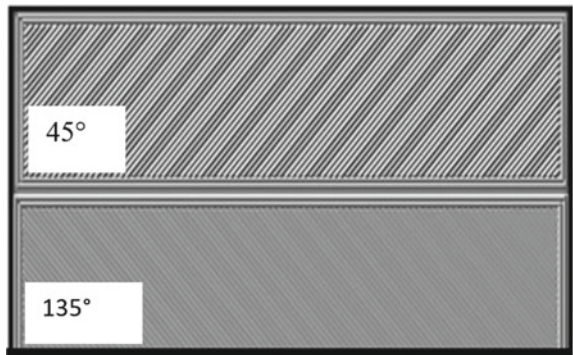
starting the printing of the specimens, it was necessary to heat the injector at 230 °C and heat the printing base to 110 °C for the ABS.

Since the printer works with interchangeable layers of 90° of separation, the 3D prints (Fig. 6) were made with filament orientation of 45° and 135° (Fig. 7 with respect to the horizontal axis, with 0.3 mm between layer and layer and filling of 90%).

The performance of mechanical tensile tests was carried out at room temperature and higher, so an electrical resistance type of band with ceramic coating (Fig. 8) was used for heat generation.

Specifications of the electrical resistance type band:

Power	950 W
Voltage	120 V
Outer diameter	80 mm
Height	60 mm

Fastening with screws

Fig. 8 Band-type electrical resistance with ceramic coating
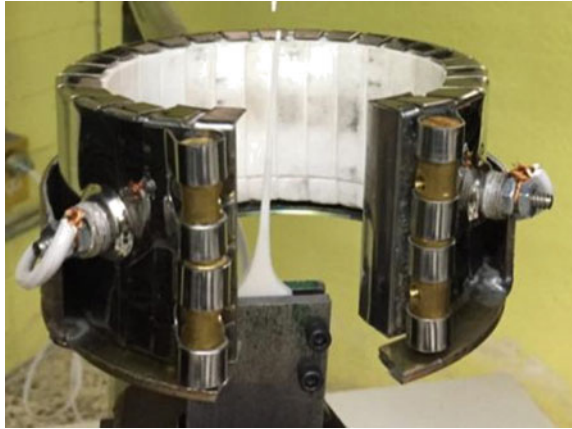
As it can be seen, there are machines with accessories to carry out thermo fluency tests, due to the lack of this type of attachments a resistance was designed as a heat source, as well as an adjustable support (Fig. 9) and independent of the universal testing machine to not interfere during the test.

The support was made of low carbon steel (mild steel), round tubular 1 ½ inch outer diameter and thin wall with vertical and horizontal sliding systems, in order to adapt to the height of the test machine.

On the horizontal axis support for the heat source was adapted, which in turn was sliding in a horizontal direction to keep the zone calibrated to the desired temperature during the tension test. Since the jaws of the test machine are very robust (Fig. 10a), an auxiliary jaw system (Fig. 10b) was adapted to not interfere with the heat source.

The jaws of the universal machine were attached to the auxiliary jaws and these in turn to the specimen by means of screws and commercial millimeter nuts.

The temperature monitoring of the ABS test tube was carried out continuously with an infrared pyrometer (Fig. 11) which allows obtaining measurements of the specimens without having to be in direct contact with it.

The tensile tests were carried out based on the standard ASTM D638, the Universal machine Shimadzu AG-I (Fig. 12) of 100 KN was used, at a constant speed of 10 mm/min.

After a series of stress tests (Fig. 13) results were obtained, and were subsequently plotted in Figure 14 and Table 2, on ABS has a higher mechanical strength at room temperature, while increasing the temperature to 35 °C this becomes more ductile but a little resistant when compared to the test at room temperature.

In the test at 45 °C the material further increases the ductility, but like the test of 35 °C its resistance decreases, as can be observed, the results are not proportional in decrease or in increment in the case of the elongations.

By increasing the temperature to 70 °C ABS becomes too ductile and its resistance decreases considerably compared to previous tests.

Fig. 9 Independent
adjustable support

Table 2 Table of results of S_y, S_u and E

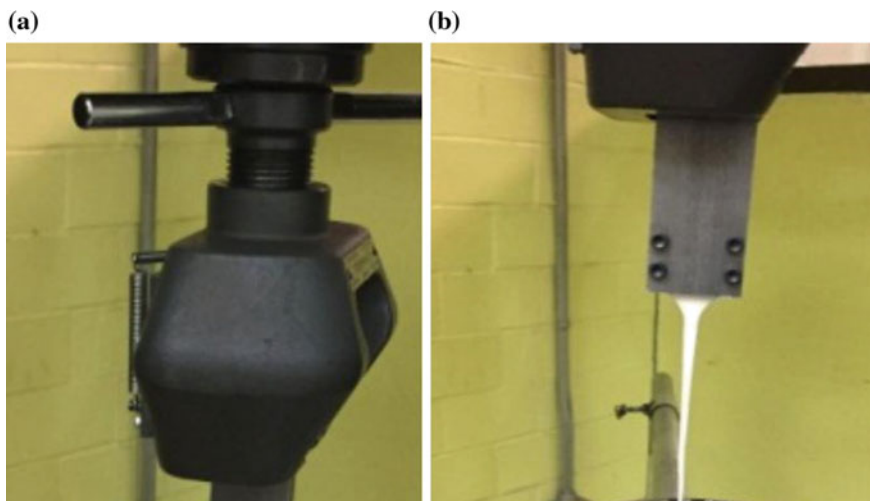| Temperature (°C)	Yield stress (S_y) (MPa)	Ultimate stress (S_u) (MPa)	Modulus of elasticity (E) (MPa)	Elongation at failure (δ) (mm)
25	30.078	32.76	1570	1.1
35	27.56	29.5	1285	1.44
45	21.72	23.41	713	1.71
70	1.17	1.35	0.517	140

Fig. 10 **a** Original jaw, **b** Auxiliary jaw

Fig. 11 Infrared pyrometer

Fig. 12 Universal tensile testing machine Shimadzu AG-I

Table 2 shows the values of the modulus of elasticity, yield stress and ultimate stress of tests at different temperatures of ABS.

5 Numerical Simulation

For numerical analysis of ABS as well as experimentation the model was developed in SolidWorks and saved with extension. IGS and subsequently exported to ANSYS.

The type of analysis was structural with static and thermal options in stable state, the discretization was based on the element Shell181, which, has been described previously.

Figure 15 shows the finite element model and the filaments of each layer with orientation angles equal to those set in 3D printing.

The mechanical properties of ABS used for numerical simulation were: modulus of elasticity (1525 MPa), Poisson ratio (0.33) and the thermal expansion coefficient $(8.2 \times 10e-5 \text{ m/M } °C)$ [14].
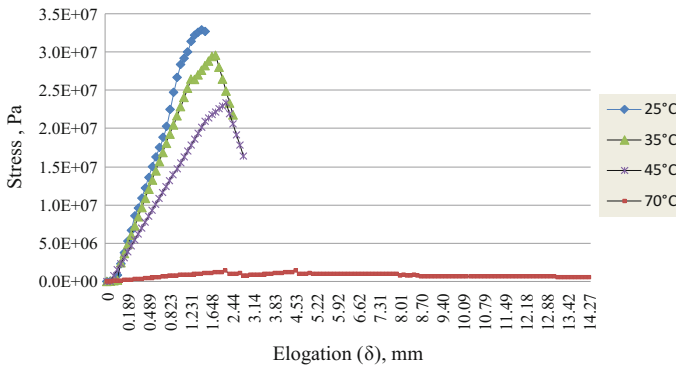
Fig. 13 ABS tensile test

Fig. 14 Thermomechanical behavior at different temperatures

The boundary conditions for the analyses performed were the constraints of displacement and rotations in the X, Y, Z axes.

The displacement generated from each of the experimental tests was introduced in each simulation.

In Figs. 16, 17, 18 and 19, the distribution of Ultimate stress (Pa) after the application of temperature and displacement is observed.

The results of each numerical analysis for each case study are set out in Table 3.
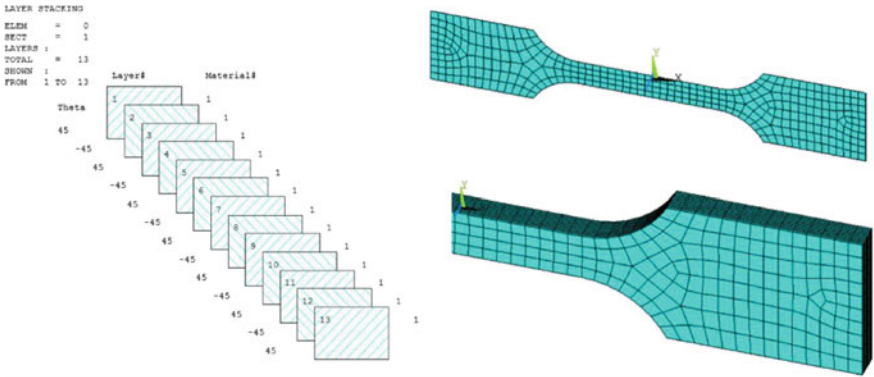
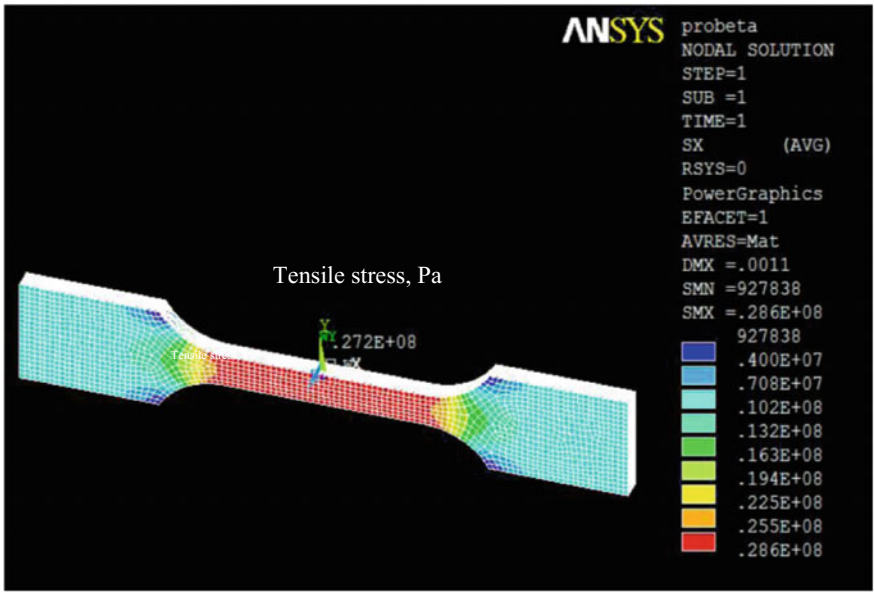**Fig. 15** Filaments oriented to 45° and 135° and finite element model

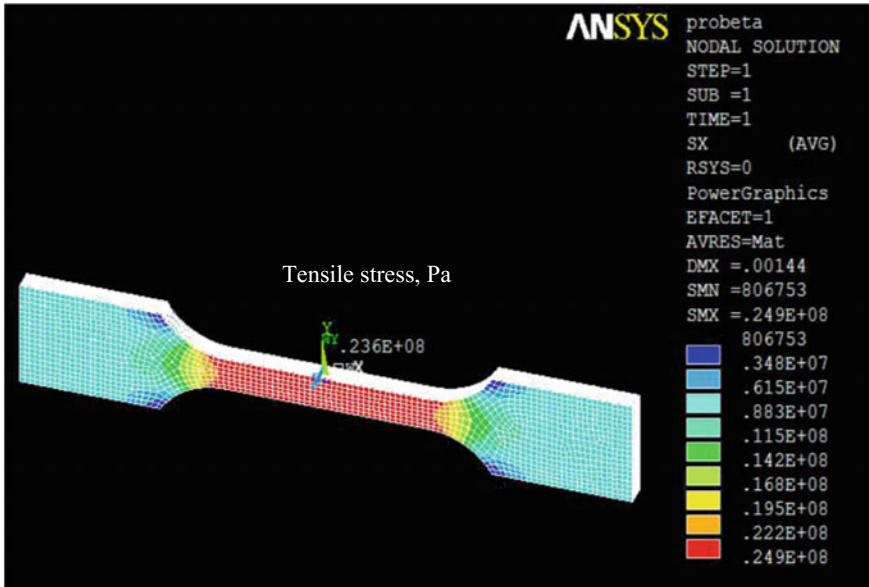**Fig. 16** Ultimate stress (Pa) distribution acting in the x-direction at 25 °C

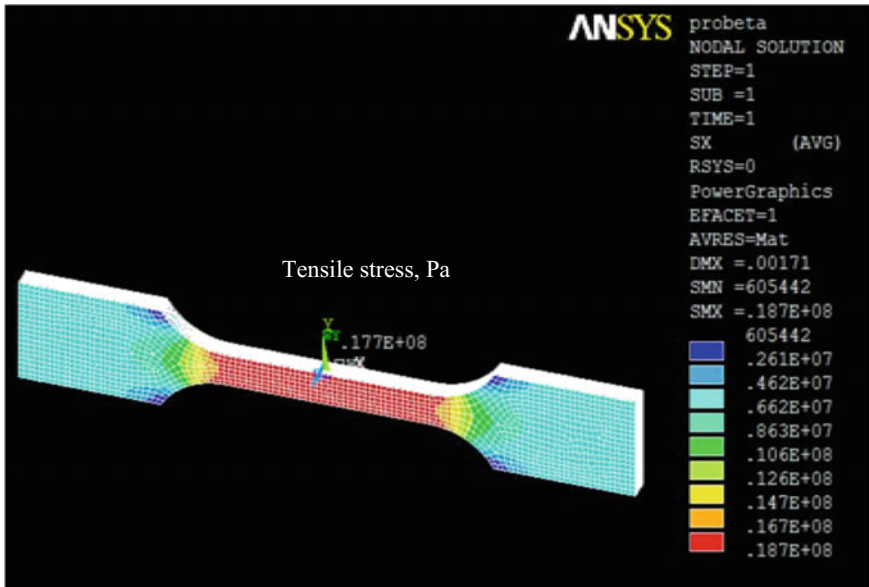**Fig. 17** Ultimate stress (Pa) distribution acting in the x-direction at 35 °C

Fig. 18 Ultimate stress (Pa) distribution acting in the x-direction at 45 °C
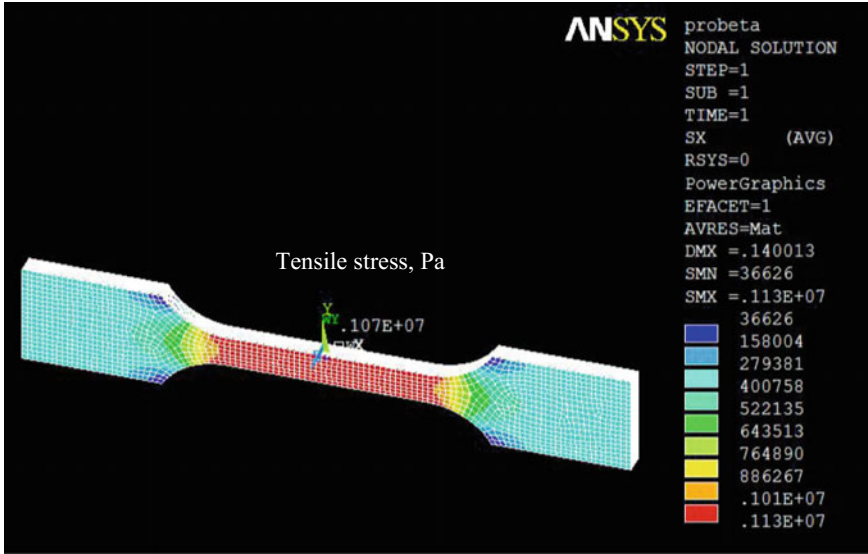
Fig. 19 Ultimate stress (Pa) distribution acting in the x-direction at 70 °C

Table 3 Stresses obtained from numerical simulations

Temperature (°C)	Ultimate stress (S_u) (MPa)	Modulus of elasticity (E) (MPa)	Elongation at failure (δ) (mm)
25	27.2	1570	1.1
35	23.6	1285	1.44
45	17.7	713	1.71
70	1.07	0.517	14

6 Conclusions

The tests performed showed results that were obtained with parameters of displacement of 10 mm/min established in universal machine tests (Shimadzu). However, these results may fall into discrepancy since there is a loss of heat because the resistance does not completely isolate the specimen from the environment.

The ABS printed specimens were based on the configuration of filaments of 45° and 135° according to results obtained in subsequent work, which show that this orientation has greater mechanical resistance.

Submitting the ABS to temperatures above the ambient implies a decrease of its resistance since the material becomes more ductile.

The experimentation of 3D printing specimens of ABS was very helpful because it provides thermo dependent data of the material such as the elastic module, in which it was of vital importance to carry out the numerical simulation.

The results of the numerical analyses compared with the experimental ones present variation, because the coefficient of thermal expansion and the Poisson relationship remained constant in each one of the analyses.

The numerical simulation is a tool of great help to carry out studies of printed pieces, since it decreased the need for prototype generation.

References

1. ASTM.: D638-10 Standard Test Method for Tensile Properties of Plastics, vol. 08.01, June (2012)
2. Guinault, A., Sollogoub, C.: Thermomechanical properties of ABS/PA and ABS/PC blends. Int. J. Mater. Form. **2**(S1), 701–704 (2009). https://doi.org/10.1007/s12289-009-0531-8
3. Artimez, J. M., Belzunce, F.J., Betegón, C., Rodriguez, C.: Estudio del comportamiento mecánico y de los micromecanismos de fractura de aceros DP mediante el uso del ensayo miniatura de punzonado. In XI Congreso Nacional de Propiedades Mecánicas de los Solidos (p. 85). Cadiz (2008)
4. Zukas, J., Zukas, V.: An introduction to 3D printing, 1st edn. First Edition Design Publishing, Sarasota, Florida (2015)
5. Cortés-Cedillo, A.R.: Caracterización mecánica de piezas de PLA fabricadas mediante impresión 3D (Master). Instituto Politécnico Nacional, ESIME Zacatenco (2016)
6. Mosca, H.O., Mastrícola, H.: Termofluencia primaria y secundaria del policloruro de vinilo. In Jornadas SAM 2000—IV Coloquio Latinoamericano de Fractura y Fatiga (pp. 001–1002). Neuquén, Argentina (2000)
7. Hernández-Palafox, E.: Estudio comparativo de las propiedades mecánicas de probetas fabricadas por procesos de manufactura de arranque de viruta y las de impresión en 3D metálicas (Master). Instituto Politécnico Nacional, SEPI ESIME Zacatenco (2016)
8. Gibson, I., Rosen, D., Stucker, B.: Additive manufacturing technologies. Springer, New York (2010)
9. Beltrán-Fernández, J.A.: Beltrán Fernández (Master). Instituto Politécnico Nacional, SEPI ESIME Zacatenco (2002)
10. Relaño-Pastor, A.A.: Estudio comparativo de piezas de ABS y PLA procesadas mediante modelado por deposición fundida (Bachelor). Universidad Carlos III de Madrid, (2013)
11. Beltrán-Fernández, J.A., Martínez-Paredes, J., González-Rebattú, M., Hernández-Gómez, L.H., Ruíz-Muñoz, O.: Customization and Numerical Simulation of a Cranial Distractor Using Computed Axial Tomography (CAT). Properties and Characterization of Modern Materials, 371–398. (2016). http://dx.doi.org/10.1007/978-981-10-1602-8_30
12. Beltrán-Fernández, J.A., Calderón, G., Camacho, N., Escalante, E., Garibaldi, P., Hernández-Gómez, L.H., Saucedo, F.: Design and manufacturing of prosthesis of a jaw for a young patient with articular ankylosis. Adv. Struct. Mater. 73–87. (2015). http://dx.doi.org/10.1007/978-3-319-19470-7_6
13. Beltran-Fernández, J.A., Gonzales-Rebatú, A.I., Hernandez-Gómez, L.H., Martínez-Paredes, J., Rangel-Elizalde, M.: Reconstruccion de fosa ocular con prótesis de hidroxiapatita y malla de titanio. Journal De Ciencia E Ingeniería **6**(1), 53–60 (2014)
14. Harper, C.: Modern Plastics Handbook, 1st edn. McGraw-Hill, New York (2000)